# Bulk matter evolution and extraction of jet transport parameters in heavy-ion collisions at energies available at the BNL Relativistic Heavy Ion Collider (RHIC)

Xiao-Fang Chen,[1,2] Carsten Greiner,[2] Enke Wang,[1] Xin-Nian Wang,[2,3] and Zhe Xu[2,4]

[1]*Institute of Particle Physics and Key Laboratory of Quark & Lepton Physics, Huazhong Normal University, Wuhan 430079, China*

[2]*Institut für Theoretische Physik, Johann Wolfgang Goethe-Universität, Max-von-Laue-Strasse 1, D-60438 Frankfurt am Main, Germany*

[3]*Nuclear Science Division, MS 70R0319, Lawrence Berkeley National Laboratory, Berkeley, California 94720, USA*

[4]*Frankfurt Institute for Advanced Studies, Ruth-Moufang-Strasse 1, D-60438 Frankfurt am Main, Germany*

(Received 19 February 2010; published 22 June 2010)

Within the picture of jet quenching induced by multiple parton scattering and gluon bremsstrahlung, medium modification of parton fragmentation functions and therefore the suppression of large transverse-momentum hadron spectra are controlled by both the value and the space-time profile of the jet transport parameter along the jet propagation path. Experimental data on single-hadron suppression in high-energy heavy-ion collisions at the Relativistic Heavy Ion Collider energy are analyzed within the higher-twist (HT) approach to the medium-modified fragmentation functions and the next-to-leading order perturbative QCD parton model. Assuming that the jet transport parameter $\hat{q}$ is proportional to the particle number density in both quark gluon plasma (QGP) and hadronic phase, experimental data on jet quenching in deeply inelastic scattering off nuclear targets can provide guidance on $\hat{q}_h$ in the hot hadronic matter. One can then study the dependence of the extracted initial value of jet-quenching parameter $\hat{q}_0$ at initial time $\tau_0$ on the bulk medium evolution. Effects of transverse expansion, radial flow, phase transition, and nonequilibrium evolution are examined. The extracted values are found to vary from $\hat{q}_0\tau_0 = 0.54$ GeV$^2$ in the $(1+3)$d ideal hydrodynamic model to 0.96 GeV$^2$ in a cascade model, with the main differences coming from the initial nonequilibrium evolution and the later hadronic evolution. The overall contribution to jet quenching from the hadronic phase, about 22%–44%, is found to be significant. Therefore, a realistic description of the early nonequilibrium parton evolution and later hadronic interaction will be critical for accurate extraction of the jet transport parameter in the strongly interacting QGP phase in high-energy heavy-ion collisions.

DOI: 10.1103/PhysRevC.81.064908 PACS number(s): 12.38.Mh, 24.85.+p, 25.75.−q

## I. INTRODUCTION

A large amount of experimental data from the Relativistic Heavy Ion Collider (RHIC) [1–4] strongly suggest that a novel form of matter, a strongly coupled quark gluon plasma (sQGP), may have been formed in the central region of high-energy heavy-ion collisions. Among the experimental evidence for the formation of sQGP are the jet-quenching phenomena that include the strong suppression of hadron spectra with large transverse momentum in central Au + Au collisions as compared to $p+p$ collisions [5,6] and the disappearance of back-to-back correlations of large transverse momentum hadrons [7]. These jet-quenching patterns observed at RHIC are in good agreement with the theoretical predictions for jet quenching [8–13] or suppression of large transverse momentum hadrons as a consequence of parton energy loss and medium-modified parton fragmentation functions induced by multiple scattering as partons propagate through the dense medium after their initial production. The parton energy loss and medium modification of the fragmentation functions owing to multiple parton scattering and induced gluon bremsstrahlung are controlled by the jet transport parameter [14],

$$\hat{q}_R = \rho \int dq_T^2 \frac{d\sigma_R}{dq_T^2} q_T^2, \tag{1}$$

or the average squared transverse momentum broadening per unit length for a jet in color representation $R$, which is also related to the gluon distribution density of the medium [14,15] and therefore characterizes the medium property as probed by an energetic jet. Here we consider a picture in which the jet parton interacts with medium particles or quasiparticles with cross section $\sigma_R$ and $\rho$ is the local particle density of the medium. Studying the jet-quenching phenomena therefore can provide important information on the space-time profile of the jet transport parameter and, consequently, properties of the sQGP in heavy-ion collisions.

Extensive phenomenological studies on the suppression of single hadron spectra [13,16–19] and dihadron correlations [20,21] at large transverse momentum have been carried out since the first observation of the strong jet-quenching phenomena. Recent emphasis of the phenomenological studies has been shifted to systematic analyses of the experimental data with different jet-quenching models and qualitative extraction of the jet transport parameter [22–26]. In this article, we carry out phenomenological analysis of the suppression of single-hadron spectra within the HT formalism for medium modification of the parton fragmentation functions and the next-to-leading order perturbative QCD parton model [20] for initial jet production. We calculate the single-hadron suppression within three different models for the dynamical evolution of the bulk matter: $(1+1)$d Bjorken model, $(1+3)$d ideal hydrodynamic model, and a parton cascade model. We study in particular the effect of collective expansion, transverse flow, nonequilibrium, and, most importantly, jet quenching in the hadronic phase of the bulk matter. Because the jet transport

 

parameter is related to the gluon distribution density of the bulk medium, one expects it to be different in a QGP and hadronic matter. We use the information on jet transport parameter in cold nuclei extracted from phenomenological studies of deeply inelastic scattering (DIS) off large nuclei [27] and extrapolate to a hot hadronic gas assuming that the gluon distribution in a nucleon in cold nuclei is the same as in a hot hadronic gas. This allows us to focus on the values of the jet transport parameter in a QGP that can be accommodated by the experimental data on single-hadron suppression and the effect of dynamic evolution of the bulk medium.

The rest of the article is organized as follows. In the next section, we review the energy loss and modified fragmentation functions in hot nuclear medium within the HT approach and their dependence on the space-time profile of the jet transport parameter $\hat{q}_R$. We then describe the next-to-leading order (NLO) pQCD parton model for single-hadron production in heavy-ion collisions in Sec. III. In Sec. IV, we introduce three different dynamic evolutions for the bulk medium. The numerical calculations and phenomenological studies of the experimental data on single-hadron suppression and extraction of the jet transport parameters within each dynamic model are carried out in Sec. V. Finally, we conclude in Sec. VI with a summary.

## II. ENERGY LOSS AND MODIFIED FRAGMENTATION FUNCTIONS

Within the generalized factorization of twist-four processes, one can calculate the nuclear modification of fragmentation functions and the energy loss of a quark propagating through nuclear matter after it is produced via a hard process in DIS off a nuclear target [28,29]. Within such HT approach, the medium modification to the quark fragmentation functions in DIS off a nuclear target is caused by multiple scattering between the struck quark and the nuclear medium on the quark's propagation path and the induced gluon bremsstrahlung, as illustrated in Fig. 1. The medium-modified quark fragmentation function,

$$\tilde{D}_q^h(z_h, Q^2) = D_q^h(z_h, Q^2) + \frac{\alpha_s(Q^2)}{2\pi}\int_0^{Q^2}\frac{d\ell_T^2}{\ell_T^2} \times \int_{z_h}^1 \frac{dz}{z}\left[\Delta\gamma_{q\to qg}\left(z, x, x_L, \ell_T^2\right) D_q^h\left(\frac{z_h}{z}\right) + \Delta\gamma_{q\to gq}\left(z, x, x_L, \ell_T^2\right) D_g^h\left(\frac{z_h}{z}\right)\right], \quad (2)$$

takes a form very similar to the vacuum bremsstrahlung corrections that lead to the Dokshitzer-Gribov-Lipatov-Altarelli-Parisi (DGLAP) [30] evolution equations in pQCD for fragmentation functions, except that the medium-modified splitting functions,

$$\Delta\gamma_{q\to qg}\left(z, x, x_L, \ell_T^2\right) = \left[\frac{1+z^2}{(1-z)_+} T_{qg}^A(x, x_L) + \delta(1-z)\Delta T_{qg}^A(x, x_L)\right]\frac{2\pi\alpha_s C_A}{\ell_T^2 N_c f_q^A(x)}; \quad (3)$$

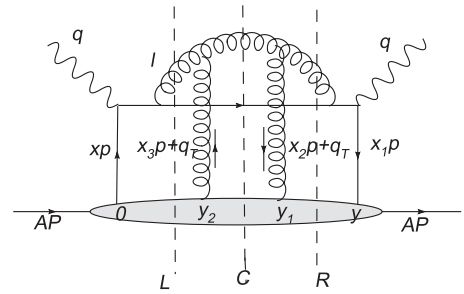


FIG. 1. A typical Feynman diagram for quark-gluon rescattering processes in DIS with three possible cuts: central (C), left (L), and right (R).

$$\Delta\gamma_{q\to gq}\left(z, x, x_L, \ell_T^2\right) = \Delta\gamma_{q\to qg}\left(1-z, x, x_L, \ell_T^2\right), \quad (4)$$

depend on the properties of the medium through the twist-four quark-gluon correlations inside the nucleus,

$$\begin{aligned} T_{qg}^A(x, x_L) &= \int\frac{d^2q_T}{(2\pi)^2}\int\frac{dy^-}{2\pi}d\xi^- dy_2^- d^2\xi_T e^{i(x+x_L)p^+y^-} \\ &\times e^{ix_T p^+\xi^- - i\vec{q}_T\vec{\xi}_T}\{(1-e^{-ix_L p^+ y_2^-})(1-e^{-ix_L p^+(y^- - y_1^-)}) \\ &+ \frac{1-z}{2}[e^{-ix_L p^+ y_2^-}(1-e^{-ix_L p^+(y^- - y_1^-)}) \\ &+ e^{-ix_L p^+(y^- - y_1^-)}(1-e^{ix_L p^+ y_2^-})]\}\theta(-y_2^-)\theta(y^- - y_1^-) \\ &\times \langle A|\bar{\psi}_q(0)\frac{\gamma^+}{2}F_\sigma{}^+(y_2^-)\,F^{+\sigma}(y_1^-, \xi_T)\,\psi_q(y^-)|A\rangle, \end{aligned} \quad (5)$$

where $\xi = y_1 - y_2$, $y$, $y_1$, and $y_2$ are space-time coordinates associated with the quark and gluon fields, as illustrated in Fig. 1. Here we include contributions beyond the helicity approximation [29] and consider only the twist-four matrices that are enhanced by the large nuclear size. The relative transverse coordinate $\xi_T$ is the Fourier conjugate of the transverse momentum $q_T$ in the gluon distribution function. The momentum fraction,

$$x_L = \frac{\ell_T^2}{2z(1-z)p^+q^-}, \quad (6)$$

is the total (+component) longitudinal momentum transfer from the target to the propagating quark and radiated gluon with longitudinal momentum $zq^-$ and transverse momentum $\ell_T$. We impose kinematic constraints $x_L \leqslant 1$ and $\ell_T \leqslant \min[zE, (1-z)E]$ in the integration in Eq. (2). A similar (+) longitudinal momentum transfer,

$$x_T = \frac{q_T^2 - 2q_T\cdot\ell_T}{2zp^+q^-}, \quad (7)$$

is also provided by the initial gluon with transverse momentum $q_T$. In the modified splitting function,

$$f_q^A(x) = \int\frac{dy^-}{2\pi}e^{ixp^+y^-}\langle A|\bar{\psi}_q(0)\frac{\gamma^+}{2}\psi_q(y^-)|A\rangle \quad (8)$$

is the quark distribution function which represents the production rate of the initial quark carrying $x = Q^2/2p^+q^-$ (the Bjorken variable) fraction of the nucleon (+) longitudinal

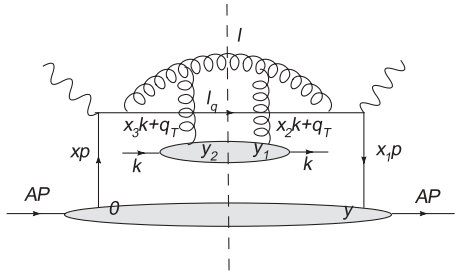


FIG. 2. Feynman diagram for induced gluon radiation in hot QGP medium that contributes the quark energy loss.

momentum in DIS. The quark-gluon matrix element,

$$\Delta T^A_{qg}(x, x_L) = \int_0^1 dz \frac{1}{1-z}\left[2T^A_{qg}(x, x_L)|_{z=1} - (1+z^2)T^A_{qg}(x, x_L)\right], \quad (9)$$

comes from the virtual correction to the induced gluon bremsstrahlung process.

If we define the quark energy loss as the energy carried by the radiative gluon in the multiple scattering processes, the total energy loss for a propagating quark in a DIS off a large nucleus is

$$\frac{\Delta E}{E} = \frac{C_A\alpha_s^2}{N_c}\int_0^{Q^2}\frac{d\ell_T^2}{\ell_T^4}\int_0^1 dz(1+z)^2\frac{T^A_{qg}(x, x_L)}{f^A_q(x)}. \quad (10)$$

One can extend the results for medium-modified parton fragmentation functions in DIS to the case of quark propagation in a hot medium (either QGP or hot hadronic matter) after it is produced through initial hard processes before the formation of the QGP [15,22] in high-energy heavy-ion collisions. In this case, we can assume the quark is produced through a hard process such as the virtual-photon-nucleus collisions in Fig. 2 and will interact with partons in the hot medium, which is independent of the initial quark production process. Therefore, we can replace the nucleus state as a product of the initial nucleus state and a thermal ensemble of quasiparticle states in the hot medium,

$$|A\rangle \to \int \frac{d^3k}{(2\pi)^3 2k^+}\psi_k(y)e^{ik\cdot y}|k\rangle \otimes |A\rangle, \quad (11)$$

and consider only the final-state interaction between the produced quark and the bulk medium, as illustrated in Fig. 2. Here $f(k, y) = |\psi_k(y)|^2$ is the local phase-space density of the quasiparticle distribution in the medium. We also neglect multiple particle correlations inside the hot medium which can be included through an effective gluon distribution density [15]. Under these assumptions, the quark-gluon correlation function in the HT approach to multiple scattering will take a factorized form,

$$\frac{T^A_{qg}(x, x_L)}{f^A_q(x)} = \frac{N_c^2-1}{4\pi\alpha_s C_R}\frac{1+z}{2}\int dy^- 2\sin^2\left[\frac{y^-\ell_T^2}{4Ez(1-z)}\right] \times \left[\hat{q}_R(E, x_L, y) + c(x, x_L)\hat{q}_R(E, 0, y)\right], \quad (12)$$

where $c(x, x_L) = f^A_q(x + x_L)/f^A_q(x)$ and $\hat{q}_R$ is the generalized jet transport parameter,

$$\hat{q}_R(E, x_L, y) = \frac{4\pi^2\alpha_s C_R}{N_c^2-1}\int\frac{d^3k}{(2\pi)^3}f(k, y) \times \int\frac{d^2q_T}{(2\pi)^2}\phi_k(x_T + x_L, q_T), \quad (13)$$

which depends on the fractional (+) longitudinal momentum transfer $x_L$ from medium gluons [31]. Here $\phi_k(x, q_T)$ is the transverse-momentum-dependent-gluon distribution function from the quasiparticle in the medium,

$$\phi_k(x, q_T) = \int\frac{d\xi^-}{2\pi k^+}d^2\xi_T\, e^{ixk^+\xi^- - i\mathbf{q}_T\cdot\xi_T} \times \langle k|F^+_\sigma(0)F^{+\sigma}(\xi^-, \xi_T)|k\rangle. \quad (14)$$

The two terms in the square brackets of Eq. (12) correspond to two different processes in the multiple scattering. The first term involves (+) longitudinal momentum transfer $x_L$ between the propagating parton and the medium owing to final gluon production. It contains what is normally defined as pure elastic energy loss [32]. The second term that is proportional to the normal (or special) transport parameter $\hat{q}_R(E, y) = \hat{q}_R(E, x_L = 0, y)$ corresponds to pure radiative processes. In this article, we assume $x \gg x_L, x_T$ and only focus on the contribution of radiative energy loss. Therefore, $c(x, x_L) \approx 1$, $\hat{q}_R(E, x_L, y) \approx \hat{q}_R(E, 0, y) \equiv \hat{q}_R(E, y)$. Given the space-time profile of the jet transport parameter $\hat{q}_R(E, y)$, one should be able to calculate the modified fragmentation function according to Eq. (2). The corresponding quark energy loss in Eq. (10) can be expressed as

$$\frac{\Delta E}{E} = \frac{N_c\alpha_s}{\pi}\int dy^- dz d\ell_\perp^2\frac{(1+z)^3}{\ell_T^4} \times \hat{q}_R(E, y)\sin^2\left[\frac{y^-l_T^2}{4Ez(1-z)}\right], \quad (15)$$

in terms of the jet transport parameter. The jet transport parameter for a gluon is 9/4 times of a quark and therefore the radiative energy loss of a gluon jet is also 9/4 times larger than that of a quark jet. In our following calculations of the hadron spectra in heavy-ion collisions, we use the same formalism for both quark and gluon modified fragmentation functions but with jet transport parameters that differ by a factor of 9/4 for quark and gluon jets.

## III. SINGLE HADRON SPECTRA WITHIN NLO PQCD PARTON MODEL

In this article, we employ the NLO pQCD parton model for the initial jet-production spectra, which has been shown to work well for large-$p_T$ hadron production in high-energy nucleon-nucleon collisions [33]. In a factorized form, the inclusive particle production cross section in $p + p$ collisions can be calculated as a convolution of parton distribution functions inside the proton, elementary parton-parton scattering

cross sections, and parton fragmentation functions,

$$\frac{d\sigma_{pp}^{h}}{dyd^2p_T} = \sum_{abcd}\int dx_a dx_b f_{a/p}(x_a,\mu^2) f_{b/p}(x_b,\mu^2) \times \frac{d\sigma}{d\hat{t}}(ab\to cd)\frac{D_{h/c}^{0}(z_c,\mu^2)}{\pi z_c} + \mathcal{O}\left(\alpha_s^3\right), \tag{16}$$

where $d\sigma/d\hat{t}(ab\to cd)$ are elementary parton scattering cross sections at leading order (LO) $\alpha_s^2$. The NLO contributions include $2\to 3$ tree-level contributions and 1-loop virtual corrections to $2\to 2$ tree processes. We refer to Ref. [20] for a detailed description. The proton parton distribution functions (PDFs) $f_{a/p}(x_a,\mu^2)$ are given by the CTEQ6M parametrization [34], where $x_a$ is the fractional momentum carried by the beam partons. The fragmentation function (FF) $D_{h/c}^{0}(z_c,\mu^2)$ of parton $c$ into hadron $h$, with $z_c$ the momentum fraction of a parton jet carried by a produced hadron are given by the updated AKK parametrization [35], which is recently improved with new input from the RHIC data, especially for $\pi^{\pm}$, $K^{\pm}$, $p/\bar{p}$, $K_S^0$, and $\Lambda/\bar{\Lambda}$ particles.

We use a NLO Monte Carlo-based program [20] to calculate the single-hadron spectra in our study. In this NLO program, the factorization scale and the renormalization scale are chosen to be the same (denoted as $\mu$) and are all proportional to the transverse momentum of the final hadron $p_T$. As pointed out in Ref. [21], the calculated single inclusive pion spectra within the NLO pQCD parton model for $p+p$ collisions agree well with the experimental data at the RHIC energy using the scale in the range $\mu = 0.9\sim 1.5p_T$. We find that the calculated $\pi^0$ spectra in $p+p$ collisions with the scale $\mu = 1.2p_T$ can fit RHIC data very well and use the same scale in $A+A$ collisions in our following calculations.

We further assume that the factorized form for large-transverse-momentum single-hadron spectra in NLO pQCD parton model can be applied to heavy-ion collisions,

$$\frac{1}{N_{\rm bin}^{AB}(b)}\frac{d\sigma_{AB}^{h}}{dyd^2p_T} = \sum_{abcd}\int dx_a dx_b f_{a/A}(x_a,\mu^2) f_{b/B}(x_b,\mu^2) \times \frac{d\sigma}{d\hat{t}}(ab\to cd)\frac{\langle \tilde{D}_c^h(z_h,Q^2,E,b)\rangle}{\pi z_c} + \mathcal{O}\left(\alpha_s^3\right), \tag{17}$$

where $N_{\rm bin}^{AB}(b)$ is the number of binary nucleon-nucleon collisions at a fixed impact $b$ of $A+B$ nuclear collisions, $\langle \tilde{D}_c^h(z_h,Q^2,E,b)\rangle$ is the medium-modified parton FF averaged over the initial production position and jet propagation direction, and $f_{a/A}(x_a,\mu^2)$ is the effective parton distributions per nucleon inside a nucleus. For large transverse momentum hadron production, the effect of nuclear modification of the parton distributions is small. We neglect such nuclear effect in our study here.

According to the definition of the jet transport parameter in Eq. (13), it should be proportional to the local particle density at $\vec{r}_j = \vec{r} + (\tau-\tau_0)\vec{n}$ in either the QGP or hadronic phase of the evolving bulk medium along the path of a propagating jet, which is a straight line in the eikonal approximation. Here $\tau_0$ is the formation time of the medium and the direction of jet propagation is defined by its azimuthal angle $\phi$ in the transverse plane. The quark-gluon correlation in Eq. (12) that enters the modified FF in Eq. (2) will involve an integration over the duration of the jet propagation and depend on the initial production position $\vec{r}$ and propagation direction $\vec{n}$. In heavy-ion collisions at a fixed impact parameter $\vec{b}$, the initial jet production cross section is proportional to the overlap function of two colliding nuclei $\int d^2r t_A(r)t_B(|\vec{b}-\vec{r}|)$. One therefore has to average over the initial jet production position and propagation direction to obtain the effective medium-modified parton FF,

$$\left\langle \tilde{D}_a^h(z_h,Q^2,E,b)\right\rangle = \frac{1}{\int d^2r t_A(|\vec{r}|)t_B(|\vec{b}-\vec{r}|)} \times \int \frac{d\phi}{2\pi} d^2r t_A(|\vec{r}|)t_B(|\vec{b}-\vec{r}|)\tilde{D}_a^h(z_h,Q^2,E,r,\phi,b). \tag{18}$$

With a given space-time profile of the jet transport parameter, one can therefore use the preceding effective medium-modified FFs to calculate the large transverse momentum hadron spectra and the the suppression factor (or nuclear modification factor),

$$R_{AB}(b) = \frac{d\sigma_{AB}^{h}/dyd^2p_T}{N_{\rm bin}^{AB}(b)d\sigma_{pp}^{h}/dyd^2p_T}, \tag{19}$$

for characterization of the effect of jet quenching on hadron spectra in heavy-ion collisions [36]. Phenomenological study of the experimental data on the preceding hadron suppression factor will in turn provide us constraints on the space-time profile of the jet transport parameter $\hat{q}_R(E,y)$.

The computation of the effective medium-modified jet FF in Eq. (18) involves a six-dimensional integration which is in addition to the Monte Carlo integration in the NLO pQCD calculation of the single-hadron spectra [20]. Numerically, we compute and tabulate the medium-modified FFs as functions of the initial jet energy $E$, fractional momentum $z$, and the factorization scale $Q^2$ for a fixed value of impact parameter $b$. We then use numerical interpolation of the table for the medium-modified FFs in the NLO pQCD calculation of the single-hadron spectra.

## IV. BULK MATTER EVOLUTION

Recent phenomenological studies [15,22–25] have focused on the initial values of the jet transport parameters as constrained by the experimental data. We study in this article the uncertainty of the extracted initial jet transport parameter owing to different models of the dynamical evolution of the bulk medium and in particular the effect of transverse expansion, flow effect, nonequilibrium, and phase transition by considering three different models for the bulk evolution. Assuming fast thermalization of the partonic matter in the initial stage of high-energy heavy-ion collisions, we consider first $(1+1)$d Bjorken [37] and $(1+3)$d [38,39] ideal

hydrodynamic evolution of the bulk matter for the calculation of medium-modified parton FFs. Inclusion of shear and bulk viscosity in the viscous hydrodynamics can affect significantly the elliptic flow or azimuthal asymmetry of the final hadron spectra at freeze-out. Their effect on the space-time profile of the bulk medium such as entropy density, however, is much smaller (on the order of a few percent) [40–43], which we neglect here in the hydrodynamic evolution of the bulk matter for the study of jet quenching. To consider nonequilibrium evolution of the bulk matter and its effect on jet quenching, we also calculate medium-modified hadron spectra with the space-time profile of parton density as given by a parton cascade model [44,45].

### A. (1 + 1)d Bjorken expansion

In a (1 + 1)d Bjorken model [37] for the bulk evolution, the system is assumed to undergo a longitudinally boost-invariant expansion with the (1 + 1)d ideal hydrodynamic equation,

$$\frac{d\epsilon}{d\tau} = -\frac{\epsilon + P}{\tau}, \tag{20}$$

where $\epsilon$ is the energy density, $P$ is the pressure, and $\tau = \sqrt{t^2 - z^2}$ is invariant time. For a massless ideal gas equation of state (EOS), the solution of the preceding ideal hydrodynamic equation leads to a time evolution of the entropy density,

$$s = s_0 \frac{\tau_0}{\tau}, \tag{21}$$

with $s_0$ the entropy density at the initial time $\tau_0$. Because the jet transport parameter $\hat{q}_R$ is directly proportional to gluon distribution density and therefore proportional to the particle number or entropy density, we assume that it will have a similar time dependence owing to longitudinal expansion. In the (1 + 1)d Bjorken model, we further neglect the transverse expansion and phase transition. Therefore, the transverse profile of the jet transport parameter will be given by the initial transverse profile of the parton density, which we assume to be proportional to the transverse density of participant nucleons according to the wounded-nucleon model of nucleus-nucleus collision [46],

$$\hat{q} = \hat{q}_0 \frac{n_{\rm part}(\vec{b}, \vec{r})}{n_{\rm part}(\vec{0}, 0)} \frac{\tau_0}{\tau}, \tag{22}$$

where $n_{\rm part}(\vec{b}, \vec{r})$ is the transverse density of participant nucleons in nucleus-nucleus collisions with impact parameter $b$,

$$n_{\rm part}(\vec{b}, \vec{r}) = t_A(|\vec{r}|)[1 - e^{-\sigma_{NN} t_A(|\vec{b} - \vec{r}|)}] + t_A(|\vec{b} - \vec{r}|)[1 - e^{-\sigma_{NN} t_A(|\vec{r}|)}], \tag{23}$$

and $\sigma_{NN}$ is the nucleon-nucleon total inelastic cross section, which is set to be $\sigma_{NN} = 42$ mb at the RHIC energy. Here $t_A(\vec{r})$ is the nuclear thickness function,

$$t_A(\vec{r}) = \int_{-\infty}^{\infty} dz\, \rho_A(\vec{r}, z), \tag{24}$$

and $\rho_A(\vec{r}, z)$ is the single-nucleon density in the nucleus normalized to $\int d^2 r t_A(\vec{r}) = A$. The total number of participant nucleons in nucleus-nucleus collisions at impact parameter $b$ is then $N_{\rm part}(b) = \int d^2 r n_{\rm part}(\vec{b}, \vec{r})$. In the space-time profile of the jet transport parameter in Eq. (22), $\hat{q}_0$ is defined as the jet transport parameter at the center of the bulk medium in the most central nucleus-nucleus collisions ($b = 0$).

We consider two different nuclear distributions for $\rho_A(\vec{r}, z)$ in the (1 + 1)d Bjorken model. One is the Woods-Saxon distribution:

$$\rho_A(\vec{r}, z) = \frac{n_0}{1 + e^{\frac{\sqrt{|\vec{r}|^2 + z^2} - R_A}{d}}}, \tag{25}$$

where $d = 0.662$ fm, $R_A = 1.26 A^{1/3}$ fm, and $n_0$ is the normalization factor given by $\int d^2 r dz\, \rho_A(\vec{r}, z) = A$ [47]. We also consider the simple hard-sphere distribution,

$$\rho_A(\vec{r}, z) = \frac{3A}{4\pi R_A^3} \theta(R_A - \sqrt{|\vec{r}|^2 + z^2}), \tag{26}$$

with $R_A = 1.12 A^{1/3}$ for comparison.

In the present work we focus on jet quenching in the 10% most central collisions. By comparing the averaged number of participating nucleons,

$$\langle N_{\rm part} \rangle = \frac{\int db\, b N_{\rm part}(b)}{\int db\, b}, \tag{27}$$

which is given by experiments for the 10% most central collisions [48], we determine the averaged value of impact-parameter $b = 3.15$ fm for Woods-Saxon nuclear distribution and $b = 2.2$ fm for the hard-sphere distribution.

### B. (1 + 3)d ideal hydrodynamical expansion

To take into account both longitudinal and transverse expansion in the ideal hydrodynamic description of the bulk matter evolution, we use the output of calculations of Hirano *et al.* [38,39] for Au + Au collision at the RHIC energy with Glauber collisions geometry and the average impact parameter $b = 3.2$ fm, corresponding to the 10% most central events. The initial condition for the (1 + 3)d ideal hydrodynamic equations is fixed such that the final bulk hadron spectra from the RHIC experiments are reproduced [38,39]. We use the code provided by Hirano [49] that interpolates the numerical data from the hydrodynamic solution on a space-time grid for energy density, temperature, flow velocity, and fraction of QGP phase.

For our purpose, we have to infer parton and hadron number density from the energy density or temperature provided by the hydrodynamic solution, which uses a bag model for the EOS [50]. In this bag model, the parton number and energy density in the QGP phase are

$$\rho^{\rm QGP} = \left(16 \frac{\zeta(3)}{\pi^2} + 36 \frac{3\zeta(3)}{4\pi^2}\right) T^3 \equiv a_1 T^3, \tag{28}$$

$$\epsilon^{\rm QGP} = \left(16 \frac{\pi^2}{30} + 36 \frac{7\pi^2}{240}\right) T^4 + B \equiv b_1 T^4 + B \tag{29}$$

for three quark flavors. The bag constant $B = (247\ \text{Mev})^4$ gives rise to a first-order phase transition from the QGP to a hadron resonance gas at the critical temperature $T_c = 170$ MeV.

In our calculation of medium-modified parton FFs, we consider jet-medium interaction in both partonic and hadronic phases throughout the evolution of the bulk matter. Neglecting hadron correlation in the medium, the jet transport parameter will be proportional to hadron density and the soft gluon distribution within each hadron. There have been several phenomenological studies [51–53] of jet quenching in DIS off large cold nuclei as measured by the HERMES [54] experiment. Within the same HT approach, the jet transport parameter is found [27] to be $\hat{q}_N \approx 0.02$ GeV$^2$/fm at the center of the cold nucleonic matter in a large nucleus. Within the HT approach and in most of the theoretical models of parton energy loss, the jet transport parameter $\hat{q}$ is an intrinsic medium property that is independent of the jet energy. A recent study in Ref. [15] predicts a weak energy dependence because of the gluon saturation in a QGP as probed by an energetic jet. In DIS off large nuclei as studied by HERMES, the typical energy of the stuck quark is about $\nu = 10$–$20$ GeV, which is roughly the same as the energy range of the initial jets that are responsible for the large-transverse-momentum hadron spectra ($p_T = 5$–$15$ GeV) as measured by the RHIC experiments. Therefore, the extracted $\hat{q}_N$ from the study [27] of HERMES data provides information on the jet transport parameter in cold nuclear matter, which can be used to estimate the $\hat{q}_h$ of hot hadronic matter in the later stage of dense-matter evolution as probed by jets at the RHIC energy, assuming $\hat{q}_h$ is proportional to the local hadron density.

In the $(1+3)$d ideal hydrodynamic model, the hadronic phase of the medium evolution is considered as a hadron resonance gas, in which the jet transport parameter can be approximate as

$$\hat{q}_h = \frac{\hat{q}_N}{\rho_N}\left[\frac{2}{3}\sum_M \rho_M(T) + \sum_B \rho_B(T)\right], \tag{30}$$

where $\rho_N = n_0 \approx 0.17$ fm$^{-3}$ is the nucleon density in the center of a large nucleus and the factor $2/3$ accounts for the ratio of constituent quark numbers in mesons and baryons. The hadron density at a given temperature $T$ and zero chemical potential is

$$\sum_h \rho_h(T) = \frac{T^3}{2\pi^2}\sum_h \left(\frac{m_h}{T}\right)^2 \sum_{n=1}^{\infty} \frac{\eta_h^{n+1}}{n} K_2\left(n\frac{m_h}{T}\right), \tag{31}$$

where $\eta_h = \pm$ for meson ($M$)/baryon ($B$). In this article, we include all hadron resonances with mass below 1 GeV. Other hadron resonance gas models normally include hadrons with mass up to 2 GeV which will only make some differences to our assumed $\hat{q}_h$ close to the phase-transition temperature.

With the preceding approximation for hadron density and jet transport parameter in the hadron phase of bulk medium evolution, the jet transport parameter throughout the evolution of the medium can be expressed as

$$\hat{q}(\tau, r) = \hat{q}_0 \frac{\rho^{\mathrm{QGP}}(\tau, r)}{\rho^{\mathrm{QGP}}(\tau_0, 0)}(1-f) + \hat{q}_h(\tau, r) f, \tag{32}$$

where $f(\tau, r)$ is the fraction of the hadronic phase at any given time and local position and $\hat{q}_0$ denotes the jet transport parameter at the center of the bulk medium in the QGP phase at the initial time $\tau_0$. To illustrate the behavior of the jet transport parameter in dense medium, we plot $\hat{q}/T^3$ in Fig. 3 as a function of the temperature $T$ according to the preceding assumptions, where we have used the initial value of $\hat{q}_0 = 0.9^{+0.05}_{-0.04}$ GeV$^2$/fm, as extracted by phenomenological study of experimental data later in this article, at an initial temperature $T_0 = 369$ MeV in the most central Au + Au collisions at RHIC. Apparently, we have neglected any additional temperature dependence beyond that in Eq. (32). Perturbative calculations [15,55] in finite-temperature QCD with resummed hard-thermal loops give rise to a logarithmic temperature dependence of $\hat{q}/T^3$ for a fixed value of the strong coupling constant $\alpha_s$. The same perturbative calculations also lead to somewhat weak jet-energy dependence of the jet transport parameter, which we neglect in this phenomenological study. Therefore, one can consider the exacted jet transport parameter as an averaged value over the range of jet energies in the experimental data.

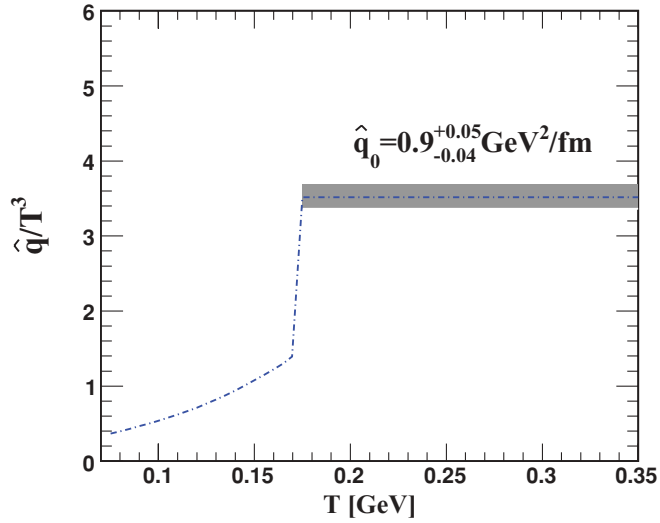


FIG. 3. (Color online) The temperature dependence of $\hat{q}/T^3$.

To study the effect of phase transition in the $(1+3)$d hydrodynamic evolution of the bulk matter in jet quenching, we set $f = 0$ in Eq. (32) and determine the parton density $\rho = a_1[(\epsilon - B)/b_1]^{3/4}$ according to Eq. (28) throughout the bulk evolution, with $\epsilon$ given by the $(1+3)$d hydrodynamic evolution at given space and time. Calculations with this prescription of space-time profile of the jet transport parameter are labeled as no phase transition in this article. We can also set $\hat{q}_0^h = 0$ to quantify the hadronic contribution to jet quenching.

The jet transport parameter $\hat{q}$ in Eq. (32) is given in the frame where the medium is at rest. To take into account of the radial flow, one can simply make the following substitute [56,57]:

$$\hat{q} \to \hat{q}\frac{p^\mu u_\mu}{p_0}, \tag{33}$$

where $p^\mu$ is the four-momentum of the jet and $u^\mu$ is the four-flow velocity in the collision frame, which is provided by the solution of the $(1+3)$d hydrodynamical equations [38,39]. Such flow dependence effectively decreases (increases) the

parton energy loss when the jet propagates along the same (opposite) direction as the flow.

### C. (1 + 3)d parton cascade

To study the effect of nonequilibrium evolution of the bulk matter on jet quenching in this article, we also consider a parton cascade model. The Boltzmann approach of multiparton scatterings (BAMPS) model [44,45] solves the Boltzmann equation for on-shell gluons with pQCD-based interactions, which include elastic scattering, bremsstrahlung, and its back reaction. The thermal equilibration process of gluons has been thoroughly investigated within this parton transport model [45,58]. BAMPS can in principle describe collective flow behavior [59–61] and the nuclear modification factor $R_{AA}$ of jet quenching [62] within a common framework.

In this work we use the output from BAMPS [60] model for central Au + Au collisions with $b = 3.4$ fm at the RHIC energy. Initial gluons or minijets are produced by binary nucleon-nucleon collisions with a Glauber geometry. The Lorentz contracted nuclei have a longitudinal extent of 0.2 fm. Thus, most minijets are produced at $t = 0.1$ fm/$c$ when two nuclei fully overlap. The strong QCD coupling constant is set to be a constant, $\alpha_s = 0.3$. Gluons freeze-out when the local energy density goes below a critical value, which is chosen as $\epsilon_c = 0.6$ GeV/fm$^3$. This corresponds to a critical temperature of $T_c = 175$ MeV in a fully equilibrated gluon gas. In the present implementation of BAMPS there is no hadronization or hadron cascade. Gluons propagate freely (free streaming) after freeze-out. During this stage we regard one gluon as one hadron according to a parton-hadron duality picture. With these setups the final transverse energy and the elliptic flow $v_2$ from BAMPS calculations agree with the experimental data at RHIC [59].

We use Eqs. (32) and (33) to evaluate the jet transport parameter in the evolving bulk medium as described by the BAMPS model. The local gluon density and flow velocity are obtained by integrating the local gluon phase space distribution given by BAMPS. The hadron fraction $f$ is either 0 before gluon freeze-out or 1 after gluon freeze-out as a simplification for the hadronization process. By setting $f = 0$ all the time, one effectively neglects the effect of phase transition and the difference in the jet transport parameter in QGP and hadronic phase. The hadron density is estimated from a free-streaming hadron gas according to an assumption of hadron-parton duality.

## V. NUMERICAL RESULTS AND COMPARISONS

With the three different models for the bulk matter evolution and the prescriptions for the evaluation of the jet transport parameter in the evolving medium as described in the preceding section, we can conduct a systematic analysis of the experimental data on suppression of high-$p_T$ hadron spectra within the HT approach to the medium-modified jet FFs. Our aim in this work is to study the theoretical uncertainties associated with the dynamical evolution of the bulk medium and effects of jet hadron interaction in the hadronic medium on jet quenching. Because we assume that the jet transport parameter in the hadronic phase can be estimated from the value as determined in the cold nuclear matter in the DIS off nuclear targets [Eq. (30)], our specific problem in this case is to determine the value of the jet transport parameter $\hat{q}_0$ at the center of the overlapped region in the central Au + Au collisions in the QGP phase at the initial time $\tau_0$ [see Eqs. (22) and (32)].

Shown in Fig. 4(a) are comparisons between the PHENIX experimental data on $R_{AA}$ for the neutral pion spectra in the 10% most central Au + Au collisions [63] at the highest RHIC energy $\sqrt{s} = 200$ GeV/$n$ and our NLO pQCD calculations with the medium-modified FFs as given in the HT approach for three different values of $\hat{q}_0$ at the initial time $\tau_0 = 0.6$ fm/$c$, using (1 + 1)d Bjorken model of ideal hydrodynamical evolution without a phase transition. The top panel of Fig. 4(a)

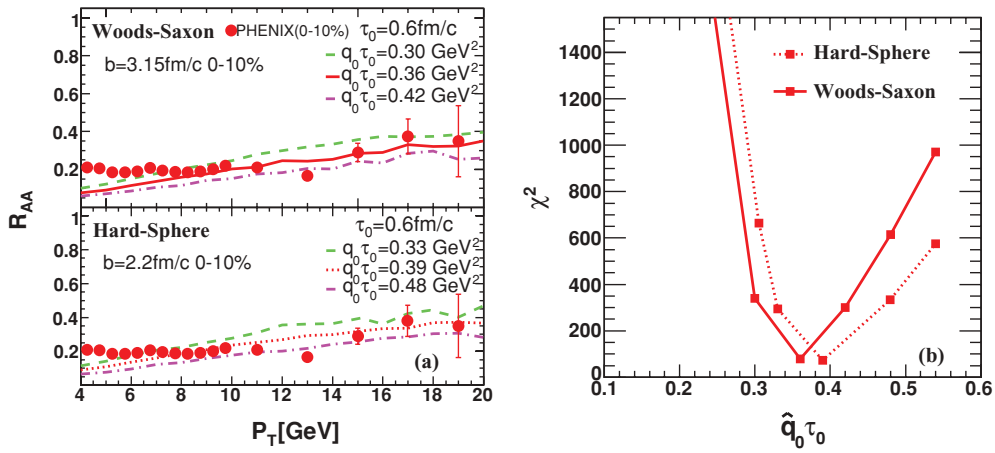


FIG. 4. (Color online) (a) Nuclear modification factor at midrapidity for the 10% most central Au + Au collisions at the maximum RHIC energy $\sqrt{s} = 200$ GeV/$n$. The symbols are the PHENIX data taken from Ref. [63]. The curves are NLO pQCD calculations with three different values of $\hat{q}_0\tau_0$ in the (1 + 1)d Bjorken model with the Woods-Saxon (top) and hard-sphere (bottom) distribution function. (b) The corresponding $\chi^2$ of the fit as a function of $\hat{q}_0\tau_0$.

shows the results with the Woods-Saxon nuclear geometry while the bottom panel is for hard-sphere nuclear distribution. The difference between the calculated suppression factors with hard-sphere and Woods-Saxon nuclear distributions is about 10%, owing to the small difference in the thickness and overlap functions with these two nuclear distributions.

In the remainder of this article, we discuss the determination of initial jet transport parameter and its uncertainties associated with the modeling of the bulk medium evolution. We carry out systematic $\chi^2$ fits to the experimental data on the suppression factor $R_{AA}$ of neutral pion spectra from the PHENIX experiment [63] with our NLO pQCD calculations that include jet quenching in an evolving bulk medium. We follow Ref. [64] to carry out a modified $\chi^2$ analysis and obtain the best-fit parameters $\hat{q}_0\tau_0$ for each model of bulk medium evolution by minimizing

$$\chi^2 = \sum_{i=1}^{N} \frac{\left[y_i + \epsilon_b \sigma_{b_i} + \epsilon_c y_i \sigma_c - y_i^{th}\right]^2}{\tilde{\sigma}_i^2} + \epsilon_b^2 + \epsilon_c^2, \quad (34)$$

$$\tilde{\sigma}_i = \sigma_i \left(\frac{y_i + \epsilon_b \sigma_{b_i} + \epsilon_c y_i \sigma_c}{y_i}\right), \quad (35)$$

of the fits with respect to two parameters $\epsilon_b$ and $\epsilon_c$, where $y_i$ is the central value of experimental data with three types of uncertainties, $\sigma_i$ (statistical plus uncorrelated systematics), $\sigma_{b_i}$ (correlated systematics), and $\sigma_c$ (normalization uncertainties) for $p_T$ larger than 6.5 GeV/$c$, and $y_i^{th}$ is the calculated results at each $p_T$ point. Shown in Fig. 4(b) as two examples are the $\chi^2$ distributions as functions of $\hat{q}_0\tau_0$ ($\tau_0 = 0.6$ fm/$c$) from the fits with the NLO pQCD calculation with (1 + 1)d Bjorken model for the bulk medium evolution. The best-fit value is $\hat{q}_0\tau_0 = 0.36$ and 0.39 GeV$^2$ for Woods-Saxon and hard-sphere nuclear distribution function, respectively. In the following calculations, we always use the Woods-Saxon nuclear distribution function.

Listed in Table I are the best-fit values of $\hat{q}_0\tau_0$ and the corresponding $\chi^2$ for jet quenching in various models for the bulk medium evolution. We discuss and compare them in detail in the remainder of this section.

TABLE I. Initial jet transport parameter $\hat{q}_0\tau_0$ and the corresponding $\chi^2$. Check signs ($\surd$) denote the inclusion of flow or phase transition (PT) in the calculations. The initial $\tau_0$ is 0.6 fm/$c$ for hydrodynamic and 0.3 fm/$c$ for BAMPS model.

| Model | Flow | PT | $\hat{q}_0\tau_0$(GeV$^2$) | $\chi^2$ |
|---|---|---|---|---|
| (1 + 1)d Bjorken [W-S] | | | 0.36 | 78 |
| (1 + 3)d Hydro | | | 0.42 | 116 |
| | $\surd$ | | 0.48 | 80 |
| | $\surd$ | $\surd$ | 0.54 | 106 |
| ($\hat{q}_0^h = 0$) | $\surd$ | $\surd$ | 0.78 | 71 |
| BAMPS | | | 0.72 | 95 |
| | $\surd$ | | 0.84 | 84 |
| | $\surd$ | $\surd$ | 0.96 | 96 |
| ($\hat{q}_0^h = 0$) | $\surd$ | $\surd$ | 1.17 | 86 |

### A. (1 + 1)d Bjorken versus (1 + 3)d ideal hydrodynamical model

We first compare the results from (1 + 1)d Bjorken and (1 + 3)d ideal hydrodynamic model with different options and study the effects of the transverse expansion, radial flow, and contributions from jet quenching in the hadronic phase. Comparing the (1 + 1)d Bjorken and (1 + 3)d ideal hydrodynamical evolution without radial flow and phase transition, it is clear that the transverse expansion cools the system considerably faster in the later stage of the evolution. This faster cooling owing to the transverse expansion leads to a faster decrease of the jet transport parameter in the (1 + 3)d hydrodynamic model than in the (1 + 1)d Bjorken model, as shown in Fig. 5 by the dot-dashed [(1 + 3)d hydrodynamics] and solid lines [(1 + 1)d Bjorken hydrodynamics]. To compensate for this faster cooling, one has to increase the value of the initial jet transport parameter $\hat{q}_0$ by 17% in the case of (1 + 3)d hydrodynamic evolution relative to the case of (1 + 1)d Bjorken expansion to fit the measured suppression factor $R_{AA}(p_T)$ for neutral pions in the central Au + Au collisions at RHIC.

Inclusion of the radial flow in the calculation of the jet transport parameter as in Eq. (33) will also change the effective jet quenching throughout the evolution of the bulk medium. Shown in Fig. 6 are the time evolution of the radial flow velocity in (1 + 3)d hydrodynamics (dashed line). The radial flow velocity in the center of the dense medium [Fig. 6(a)], where jet quenching is the strongest, remains small, at about 0.2, throughout hydrodynamic expansion. In the same figure, we also plot the fraction of the hadron phase (solid lines) as a function of time in the (1 + 3)d hydrodynamics. The period between $f = 0$ and $f = 1$ indicate the duration of the phase transition or the mixed phase. We notice that at the beginning of the mixed phase the radial flow velocity starts to saturate and even decrease a little. This is mainly attributable to the mass effect. The energy, approximately $m_T v$, where $m_T$ is the transverse mass, should be the same during the phase transition. Therefore, the radial flow velocity will decrease as particles become massive during the phase transition. Such decrease will be partially compensated by

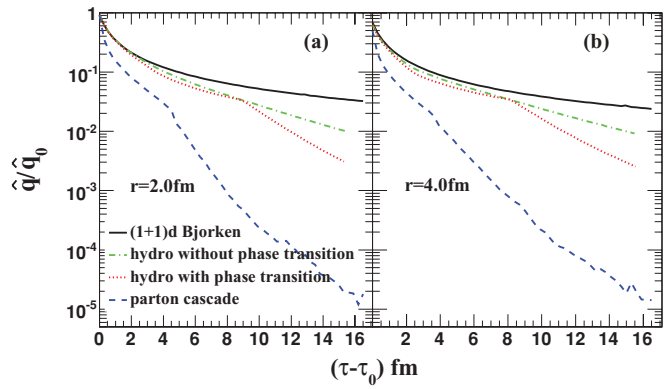


FIG. 5. (Color online) Time evolution of the scaled jet transport parameter at position of radius of 2 fm (a) and 4 fm (b) for various models of the bulk matter evolution. The flow effect in Eq. (33) is not included.

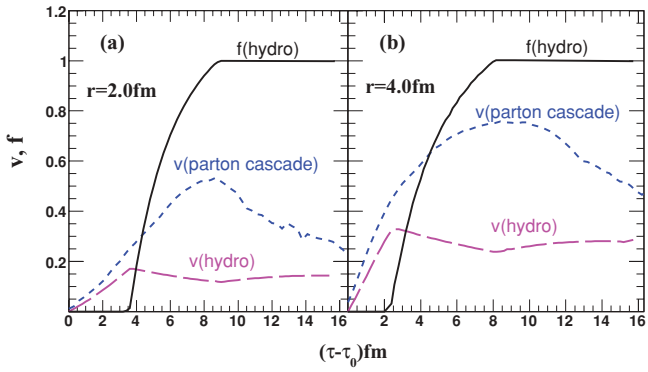


FIG. 6. (Color online) The radial flow velocity in the $(1 + 3)$d hydrodynamical model and the parton cascade at position of radius of 2 fm (a) and 4 fm (b). The solid curves show the fraction of the hadron phase in the hydrodynamical model.

the continued collective expansion, which tends to increase the flow velocity. As the phase transition is completed, the radial flow velocity should increase again by further transverse expansion in the hadronic phase and the resonances decays.

The radial flow will reduce the effective jet transport parameter $\hat{q}$ if jets propagate along with it and increase the effective value of $\hat{q}$ if jets propagate against it. After averaging over the direction and initial position of jet production, the effective jet transport parameter is merely reduced by less than 14% [56]. As shown in Table I, this leads to an increase of $\hat{q}_0$ about 14% when one includes the effect of radial flow in the $(1 + 3)$d hydrodynamic evolution in fitting experimental data on $R_{AA}(p_T)$.

In $(1 + 1)$d Bjorken and two options of the $(1 + 3)$d hydrodynamic expansion as discussed earlier, we have neglected the difference of the jet transport parameters in QGP and hadronic phases. These options are labeled as no phase transition (PT) by setting $f = 0$ in Eq. (32) and using $\rho^{\rm QGP} = a_1[(\epsilon - B)/b_1]^{3/4}$ in Eq. (28) throughout the evolution even in the mixed and hadronic phases.

In the realistic scenario, jet transport parameter $\hat{q}_h$ in the hadronic phase should be different from that in the QGP phase and we assume that $\hat{q}_h$ is proportional to $\hat{q}_N$ in the cold nuclear medium and the hadron number density as in Eq. (30). With this assumption, there is a discontinuity in $\hat{q}$ as a function of time (or temperature as in Fig. 3) at the end of the mixed phase, as show by the dotted lines in Fig. 5, and the jet transport parameter in the hadronic phase in the later stage of the bulk medium evolution will be smaller than the scenario of no PT in the $(1 + 3)$d hydrodynamics. Therefore, one needs a larger value of the initial jet transport parameter $\hat{q}_0$, about 13%, to account for the measured suppression factor $R_{AA}(p_T)$ as compared to an evolving bulk medium with the same jet transport parameter throughout difference phases.

To determine the contribution of jet quenching in the hadronic phase, we set $\hat{q}_0^h = 0$ in Eq. (32), assuming parton energy loss only happens in the QGP phase. In this case, the extracted $\hat{q}_0$ will be about 44% larger (see Table I). This implies that the hadronic phase contributes to about 44% of the total suppression of the high-$p_T$ hadron spectra. Such a large contribution is attributable to the lifetime of the mixed and hadronic phases until the kinetic freeze-out, which is longer than the lifetime of the QGP phase, though the hadron density is much smaller than the initial parton density in the QGP phase. A better understanding of the hadronic contribution to the jet quenching is, therefore, important for an accurate extraction of the jet transport parameter in the initial phase of strongly interacting QGP.

### B. (1 + 3)d parton cascade versus (1 + 3)d ideal hydrodynamical model

In a parton cascade model such as BAMPS, the system takes times to reach thermal or partial thermal equilibrium after the initial parton production time, $\tau_0 = 0.3$ fm/$c$. During this period of parton equilibration, there is entropy production accompanied by rapid expansion. The net effect is a much faster decreasing of the effective temperature [44,45,65] and the parton density during the early stage of the bulk medium evolution. The corresponding jet transport parameter in the equilibrating gluonic matter in BAMPS calculation therefore decreases much faster than that in both $(1 + 1)$d and $(1 + 3)$d ideal hydrodynamic models in the early stage of evolution, as shown by the dashed lines in Fig. 5. It is smaller by more than a factor of 2 before the hadronization. This leads to about 77% increase in the initial value of $\hat{q}_0$ that is needed to account for the measured suppression of hadron spectra (see Table I). Note that in our calculations jet quenching starts at the thermalization $\tau_0 = 0.6$ fm/$c$ in the ideal hydrodynamic model. However, it starts at $\tau_0 = 0.3$ fm/$c$ in the BAMPS model immediately after the initial gluons are produced and before thermal or partial thermal equilibrium is reached. Such jet medium interaction and parton energy loss during the thermalization stage in the BAMPS model will contribute to some additional, though a small fraction, suppression of the final hadron spectra.

In BAMPS, the hadronization of the gluonic matter happens when the local gluon energy density is below $\epsilon_c = 0.6$ GeV/fm$^3$ and parton-hadron duality is used for the phase-space density of hadrons, which are assumed to freeze-out immediately. Such a sudden hadronization and freeze-out scenario implies the change of the hadron fraction $f$ from 0 to 1 at this critical density in the evaluation of the jet transport parameter in Eq. (32). The lack of the mixed phase in BAMPS, which lasts for about 5–6 fm/$c$ in the $(1 + 3)$d ideal hydrodynamic evolution, as indicated by the duration for the hadron fraction to reach $f = 1$ in Fig. 6, leads to smaller value of the jet transport parameter after the hadronization. Comparing the extracted values of $\hat{q}_0$ from the phenomenological fit with and without ($\hat{q}_h = 0$) hadronic phase, as shown in Table I, the hadronic interaction in BAMPS model contributes to about 22% of the jet quenching effect, which is about a factor of 2 smaller than that in the $(1 + 3)$d ideal hydrodynamical model.

The large viscous effect in the parton cascade model [59] generally leads to larger radial flow velocity than that generated by an ideal hydrodynamic expansion, as shown in Fig. 6. The free-streaming of hadrons immediately after the hadronization also leads to the further increase of the flow velocity. Such

larger radial flow velocity in the BAMPS model reduces the effective jet-quenching parameter and therefore leads an increase of about 16% in the extracted initial $\hat{q}_0$.

The decrease of the radial flow velocity at late times seen in Fig. 6 is a numerical artifact, which comes from the chosen geometry of spatial elements, where particles are collected to calculate the radial flow velocity. Longitudinal length of each spatial element corresponds to a space-time rapidity window $|\eta| < 0.25$, while the transverse length is fixed to be 0.3 fm. At late times the longitudinal length is larger than the transverse one, and particles with smaller transverse velocity (larger longitudinal velocity) make up the main part of the remaining particles in the spatial elements. This is the reason for the observed decrease of the radial flow velocity. If we choose the longitudinal length being equal to the transverse one at the late times, we would see a continuous increase of the flow velocity owing to the free streaming, before all particles go out of the spatial element. This is, however, a negligible effect on the extraction of $\hat{q}_0$ because the hadron density is tiny at late times.

## VI. CONCLUSIONS

Using medium-modified FFs from the HT approach to multiple parton scattering, we have calculated single inclusive hadron spectra in NLO perturbative QCD parton model. The medium modification to the FF is very similar in form to the DGLAP correction owing to vacuum gluon bremsstrahlung, except that the medium-modified splitting function contains information about the properties of the medium through a path-integrated jet transport parameter $\hat{q}$. Therefore, the medium-modified FF will explicitly depend on the space-time evolution of the bulk medium. We have focused our attention on the dependence of the medium modified FF on the space-time evolution of the bulk medium and their influence on the suppression of the single-hadron spectra at large $p_T$.

We specifically considered the effects of transverse expansion, radial flow, jet quenching in hadronic phase, and nonequilibrium effect with three different models for the bulk matter evolution in central Au + Au collisions at the RHIC energy: (1 + 1)d Bjorken hydrodynamic model, (1 + 3)d ideal hydrodynamical model by Hirano [38,39], and (1 + 3)d BAMPS [44,45] parton cascade model. Because the jet transport parameter is proportional to the particle gluon distribution density of the medium, we have assumed that it will be proportional to the local particle density in both QGP and hadronic phase during the bulk matter evolution. The coefficient of the particle density dependence, which is related to soft gluon distribution per particle, will be different in the QGP and hadronic phase. Assuming a similar density dependence of the jet transport parameter in the hadronic phase as that in large cold nuclei, but rescaled by the local hadron density and the number of constituent quarks, the only free parameter in the space-time profile is the initial value of the jet transport parameter $\hat{q}_0$ at initial time $\tau_0$ at the center of the QGP medium in central heavy-ion collisions. We have extracted values of $\hat{q}_0$ at $\tau_0$ in each model of bulk evolution with different options by fitting the experimental data on the suppression factor $R_{AA}(p_T)$ for high-$p_T$ neutral pions and studied the uncertainties in the extracted value of $\hat{q}_0$.

By comparing the values of $\hat{q}_0$ extracted with different options in models for the bulk matter evolution, we also found that the transverse expansion leads to fast cooling of the hot medium and therefore reduces jet quenching in the later stage of the evolution by about 17%. Radial flow also reduces the effective jet transport parameter by 15%. The PT from QGP to hadronic medium further reduces the effective jet transport parameter in the hadronic phase and leads to about 13% reduction of jet-quenching effect. Within our model for the form of jet transport parameter owing to jet-hadron interaction, the overall contribution to jet quenching from hadronic phase is about 22%–44%, depending on the model for evolution of the hadronic phase.

In the HT approach, gluons in the jet-medium scattering (which give rises to induced gluon radiation) can come from different sources. When they are direct thermal partons (with thermal distribution), the corresponding processes become Compton scattering and lead directly to elastic energy loss, as shown in Ref. [32]. Such contribution is included but not limited to the first term in Eq. (12). The second terms correspond to the true inelastic processes, where the medium gluons in the HT approach are from radiated processes of thermal target partons. In our current study, we lump these processes together. The fractional contributions from elastic and inelastic processes in HT approach might be different from other studies that explicitly separate elastic and inelastic processes; therefore, the values of extracted $\hat{q}_0$ should also be slightly different.

By comparing (1 + 3)d ideal hydrodynamic and the BAMPS parton cascade model, we found that the nonequilibrium evolution in the early stage of parton cascade leads to faster decrease of the jet transport parameter with time and therefore affects the overall jet quenching the most, by 77%, part of which is caused by the lack of mixed phase in the parton cascade model. Such uncertainties can be further reduced by combining parton cascade and hadron cascade with a model of of hadronization that can reproduce the EOS during the PT as given by a lattice QCD calculation.

## ACKNOWLEDGMENTS

We thank T. Hirano for providing numerical results of (1 + 3)d ideal hydrodynamic evolution of the bulk matter in heavy-ion collisions at RHIC and discussions. This work is supported by the NSFC of China under Project Nos. 10825523 and 10635020, by MOE of China under Project No. IRT0624, by MOST of China under Project No. 2008CB317106, and by MOE and SAFEA of China under Project No. PITDU-B08033, and by the Director, Office of Energy Research, Office of High Energy and Nuclear Physics, Divisions of Nuclear Physics, of the US Department of Energy under Contract No. DE-AC02-05CH11231. The numerical calculations were performed at the Center for Scientific Computing of Goethe University. This work was financially supported by the Helmholtz International Center for FAIR within the framework

of the LOEWE program (Landes-Offensive zur Entwicklung Wissenschaftlich-ökonomischer Exzellenz) launched by the State of Hesse, Germany. X.-N. Wang is grateful for the hospitality of the Institut für Theoretische Physik, Johann Wolfgang Goethe-Universität, and support by the ExtreMe Matter Institute EMMI in the framework of the Helmholtz Alliance Program of the Helmholtz Association (HA216/EMMI) during the completion of this work.

[1] I. Arsene *et al.* (BRAHMS Collaboration), Nucl. Phys. A **757**, 1 (2005).
[2] B. B. Back *et al.*, Nucl. Phys. A **757**, 28 (2005).
[3] J. Adams *et al.* (STAR Collaboration), Nucl. Phys. A **757**, 102 (2005).
[4] K. Adcox *et al.* (PHENIX Collaboration), Nucl. Phys. A **757**, 184 (2005).
[5] J. Adams *et al.* (STAR Collaboration), Phys. Rev. Lett. **91**, 072304 (2003); **91**, 172302 (2003).
[6] S. S. Adler *et al.* (PHENIX Collaboration), Phys. Rev. Lett. **91**, 072301 (2003).
[7] C. Adler *et al.* (STAR Collaboration), Phys. Rev. Lett. **90**, 082302 (2003).
[8] X. N. Wang and M. Gyulassy, Phys. Rev. Lett. **68**, 1480 (1992).
[9] M. Pluemer, M. Gyulassy, and X. N. Wang, Nucl. Phys. A **590**, 511C (1995).
[10] X. N. Wang, Phys. Rev. C **61**, 064910 (2000).
[11] X. N. Wang, Phys. Rev. C **63**, 054902 (2001).
[12] M. Gyulassy, I. Vitev, and X. N. Wang, Phys. Rev. Lett. **86**, 2537 (2001).
[13] X. N. Wang, Phys. Lett. B **579**, 299 (2004).
[14] R. Baier, Y. L. Dokshitzer, A. H. Mueller, S. Peigne, and D. Schiff, Nucl. Phys. B **484**, 265 (1997).
[15] J. Casalderrey-Solana and X. N. Wang, Phys. Rev. C **77**, 024902 (2008).
[16] I. Vitev and M. Gyulassy, Phys. Rev. Lett. **89**, 252301 (2002).
[17] X. N. Wang, Phys. Lett. B **595**, 165 (2004).
[18] K. J. Eskola, H. Honkanen, C. A. Salgado, and U. A. Wiedemann, Nucl. Phys. A **747**, 511 (2005).
[19] T. Renk, Phys. Rev. C **74**, 024903 (2006).
[20] N. Kidonakis and J. F. Owens, Phys. Rev. D **63**, 054019 (2001); B. W. Harris and J. F. Owens, *ibid.* **65**, 094032 (2002).
[21] H. Zhang, J. F. Owens, E. Wang, and X. N. Wang, Phys. Rev. Lett. **98**, 212301 (2007); J. Phys. G **34**, S801 (2007).
[22] A. Majumder, C. Nonaka, and S. A. Bass, Phys. Rev. C **76**, 041902 (2007).
[23] S. A. Bass, C. Gale, A. Majumder, C. Nonaka, G. Y. Qin, T. Renk, and J. Ruppert, Phys. Rev. C **79**, 024901 (2009).
[24] S. A. Bass, C. Gale, A. Majumder, C. Nonaka, G. Y. Qin, T. Renk, and J. Ruppert, J. Phys. G **35**, 104064 (2008).
[25] G. Y. Qin and A. Majumder, arXiv:0910.3016 [hep-ph].
[26] N. Armesto, M. Cacciari, T. Hirano, J. L. Nagle, and C. A. Salgado, J. Phys. G **37**, 025104 (2010).
[27] W. T. Deng and X. N. Wang, Phys. Rev. C **81**, 024902 (2010).
[28] X. F. Guo and X. N. Wang, Phys. Rev. Lett. **85**, 3591 (2000); X. N. Wang and X. F. Guo, Nucl. Phys. A **696**, 788 (2001).
[29] B. W. Zhang and X. N. Wang, Nucl. Phys. A **720**, 429 (2003).
[30] Y. L. Dokshitzer, Sov. Phys. JETP **46**, 641 (1977) [Zh. Eksp. Teor. Fiz. **73**, 1216 (1977)]; V. N. Gribov and L. N. Lipatov, Sov. J. Nucl. Phys. **15**, 438 (1972) [Yad. Fiz. **15**, 781 (1972)]; G. Altarelli and G. Parisi, Nucl. Phys. B **126**, 298 (1977).
[31] A. Majumder (private communication). Note that the definition of the jet transport parameter $\hat{q}_R$ used here differs from that in Ref. [22] by a factor of $\pi$. Therefore, one has to multiply values of $\hat{q}_R$ extracted from experimental data in this study by a factor of $\pi$ when compared to that in Ref. [22].
[32] X. N. Wang, Phys. Lett. B **650**, 213 (2007).
[33] J. F. Owens, Rev. Mod. Phys. **59**, 465 (1987).
[34] H. L. Lai *et al.* (CTEQ Collaboration), Eur. Phys. J. C **12**, 375 (2000).
[35] S. Albino, B. A. Kniehl, and G. Kramer, Nucl. Phys. B **803**, 42 (2008).
[36] E. Wang and X. N. Wang, Phys. Rev. C **64**, 034901 (2001).
[37] J. D. Bjorken, Phys. Rev. D **27**, 140 (1983).
[38] T. Hirano, U. W. Heinz, D. Kharzeev, R. Lacey, and Y. Nara, Phys. Lett. B **636**, 299 (2006).
[39] T. Hirano, U. W. Heinz, D. Kharzeev, R. Lacey, and Y. Nara, Phys. Rev. C **77**, 044909 (2008).
[40] D. Teaney, Phys. Rev. C **68**, 034913 (2003).
[41] P. Romatschke and U. Romatschke, Phys. Rev. Lett. **99**, 172301 (2007).
[42] H. Song and U. W. Heinz, Phys. Rev. C **77**, 064901 (2008).
[43] K. Dusling and D. Teaney, Phys. Rev. C **77**, 034905 (2008).
[44] Z. Xu and C. Greiner, Phys. Rev. C **71**, 064901 (2005).
[45] Z. Xu and C. Greiner, Phys. Rev. C **76**, 024911 (2007).
[46] A. Bialas, M. Bleszynski, and W. Czyz, Nucl. Phys. B **111**, 461 (1976).
[47] N. Schwierz, I. Wiedenhover, and A. Volya, arXiv:0709.3525 [nucl-th].
[48] J. Adams *et al.* (STAR Collaboration), Phys. Rev. C **72**, 014904 (2005).
[49] T. Hirano (private communication).
[50] C. Nonaka, E. Honda, and S. Muroya, Eur. Phys. J. C **17**, 663 (2000).
[51] E. Wang and X. N. Wang, Phys. Rev. Lett. **89**, 162301 (2002).
[52] A. Majumder, E. Wang, and X. N. Wang, Phys. Rev. Lett. **99**, 152301 (2007).
[53] A. Majumder, arXiv:0901.4516 [nucl-th].
[54] A. Airapetian *et al.* (HERMES Collaboration), Nucl. Phys. B **780**, 1 (2007).
[55] X. N. Wang, Phys. Lett. B **485**, 157 (2000).
[56] R. Baier, A. H. Mueller, and D. Schiff, Phys. Lett. B **649**, 147 (2007).
[57] H. Liu, K. Rajagopal, and U. A. Wiedemann, Phys. Rev. Lett. **97**, 182301 (2006).
[58] A. El, Z. Xu, and C. Greiner, Nucl. Phys. A **806**, 287 (2008).
[59] Z. Xu, C. Greiner, and H. Stöcker, Phys. Rev. Lett. **101**, 082302 (2008).
[60] Z. Xu and C. Greiner, Phys. Rev. C **79**, 014904 (2009).
[61] I. Bouras *et al.*, Phys. Rev. Lett. **103**, 032301 (2009).
[62] O. Fochler, Z. Xu, and C. Greiner, Phys. Rev. Lett. **102**, 202301 (2009).
[63] A. Adare *et al.* (PHENIX Collaboration), Phys. Rev. Lett. **101**, 232301 (2008).
[64] A. Adare *et al.* (PHENIX Collaboration), Phys. Rev. C **77**, 064907 (2008).
[65] T. S. Biro, E. van Doorn, B. Muller, M. H. Thoma, and X. N. Wang, Phys. Rev. C **48**, 1275 (1993).